

1

## Supplementary information

2

# Mass transfer analysis of Boron-doped Carbon Nanotubes

3

## Cathode for Dual-electrolyte Lithium-air Batteries

4 Yuyang Wang<sup>a</sup>, Mingfu Yu<sup>a</sup>, Jie Li<sup>a</sup>, Tianyu Zhang<sup>a</sup>, Xun Wang<sup>b</sup>, Milong Hao<sup>a</sup>, Xue Wang<sup>a</sup>, Long  
5 Cheng<sup>a</sup>, Hong Sun<sup>\*a</sup>

---

6 a. School of Mechanical Engineering, Shenyang Jianzhu University, 110168

7 Shenyang, China. Email: [sunhongwxh@sina.com](mailto:sunhongwxh@sina.com)

8 b. School of Science, Shenyang Jianzhu University, 110168 Shenyang, China

9 110168 Shenyang, China

10

11 **Corresponding author:** [sunhongwxh@sina.com](mailto:sunhongwxh@sina.com), [mingfuyu503@163.com](mailto:mingfuyu503@163.com)

12

13

14

15

16

17

18

19

20

21

22

23

24

25

### 1. Modeling part

26

### 2. Analysis

27

28

29

30

31

32

33

34

35

36

37

38

39

40

41

42

43

44

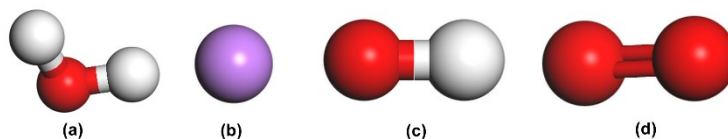
45

46

47

48

1 **1. Modeling part**  
2 **1.1 molecular dynamics**



5 Fig. S1 Microscopic particles: (a)H<sub>2</sub>O, (b)Li<sup>+</sup>, (c)OH<sup>-</sup>, (d)O<sub>2</sub>.

6

7 The Universal force field was adopted in the model, the biggest advantage of  
8 which is full element coverage. The H<sub>2</sub>O molecular model is an SPC/E model where  
9 the intermolecular forces were approximated by the Leonard-Jones potential and  
10 electrostatic interactions.

$$U_{ij} = 4\epsilon_{ij} \left[ \left( \frac{\sigma_{ij}}{r_{ij}} \right)^{12} - \left( \frac{\sigma_{ij}}{r_{ij}} \right)^6 \right] + \sum_i \sum_j \frac{q_i q_j}{r_{ij}} \quad (1)$$

11 Where  $q_i$  and  $q_j$  are the charge of the  $i^{\text{th}}$  and  $j^{\text{th}}$  particle respectively,  $r_{ij}$  is the distance  
12 between particle  $i$  and particle  $j$ ,  $\epsilon_{ij}$  is the potential well depth of particle,  $\sigma_{ij}$  is the  
13 effective distance of particle. Parameters of each particle are shown in **Table S1**.  $m$  is  
14 the relative atomic mass of atom.

15

16 Table S1 Particle parameters.

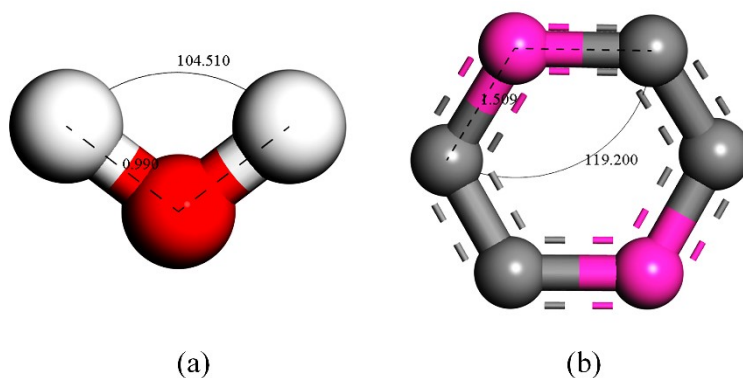
Name		$\epsilon/(\text{KJ}\cdot\text{mol}^{-1})$	$\sigma/\text{nm}$	$m$	$q/e$
H <sub>2</sub> O	Ow	0.65	0.3166	16	-0.84
	Hw	0	0	1	+0.42
LiOH	OH	0.251	0.275		-1.1029
	Li	0.5	0.30	6.9	+0.6791
O <sub>2</sub>	O	0.65	0.3166	16	0

17

18

19

1 The calculated water molecular bond length and bond angle are shown in Fig. 1(a).  
2 The bond length of O-H is 0.990 Å, the bond angle of H-O-H is 104.510 °. They are  
3 consistent with the conclusion of Zhou<sup>1</sup> et al and the experimental results. For BC<sub>3</sub>, the  
4 calculated bond length of B-C is 1.509 Å, the calculated bond angle of C-B-C is 119.2  
5 °. As Fig. 1(b), they are consistent with the conclusion of Seifollah<sup>2</sup> et al. Therefore,  
6 Universal force field is reliable for our system.



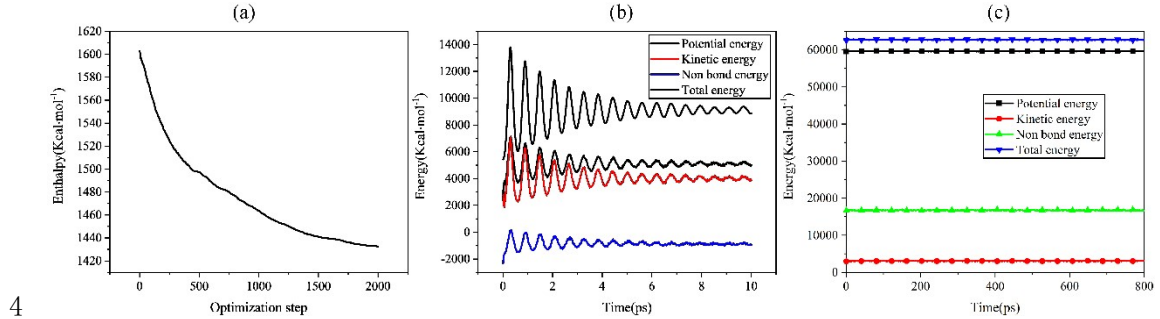
7

8

Fig.1 (a) Model of H<sub>2</sub>O, (b) Structure of the ring.

9 The model was geometrically optimized, relaxed, and annealed to obtain a  
10 relatively stable structure after it was established. The energy of the system was the  
11 lowest, and the structure was relatively stable. This article used molecular dynamics to  
12 simulate the particle motion process and uses isothermal molecular dynamics  
13 simulation based on the Nosé-Hoover temperature-controlled NVT ensemble method.  
14 The relaxing time step was 0.1 fs, and the total simulation time was 10 ps. The  
15 molecular dynamics time step was 1 fs, and the total simulation time was 800 ps. The  
16 Edward method was used for electrostatic interactions. For the intermolecular force  
17 were needed to calculate, that was, the van der Waals interaction force, the cutoff  
18 method used Atom-based cutoffs. Fig. 2 showed the energy changes during geometric  
19 optimization, relaxation and molecular dynamics. In the process of geometric

1 optimization, the energy was gradually reduced to make the body shape more stable. It  
 2 could be seen from the energy change of the relaxation process and the dynamic process  
 3 that they both reached convergence.



4  
 5 Fig. 2 Energy change process: (a) geometric optimization, (b) relaxation, (c) molecular dynamics.  
 6

7 In this paper, according to Einstein's equation, the diffusion coefficient was  
 8 calculated by means of the mean square displacement (MSD) analysis method:

$$MSD(\Delta t) = \frac{1}{\tau - \Delta t} \int_0^{\tau - \Delta t} [r(t - \Delta t) - r(t)]^2 dt = \langle [r(t - \Delta t) - r(t)]^2 \rangle \quad (2)$$

9

$$D = \frac{1}{6} \lim_{\Delta t \rightarrow \infty} \frac{dMSD}{d\Delta t} \quad (3)$$

10 Among them,  $r(t)$  represents the coordinates of the molecule at time  $t$ ,  $r(t+\Delta t)$  represents  
 11 the coordinates of the molecule at time  $t+\Delta t$ ,  $[r(t-\Delta t)-r(t)]^2$  is the mean square  
 12 displacement, and  $\tau$  is Total simulation time,  $N$  represents the total number of  
 13 molecules.

14 Radial distribution function calculation formula :

$$\rho g(r) 4\pi r^3 = dN \quad (4)$$

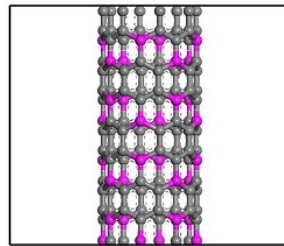
15  $\rho$  is the density of the system, when the number of molecules in the system is  $N$ :

$$\int_0^{\infty} \rho g(r) 4\pi r^3 = \int_0^N dN = N \quad (5)$$

1

## 2 1.2 DFT calculation

3 The calculation method of the diffusion energy barrier of particles (such as  
4 sidewall) is: First, placing the particles outside the nanotube, directly above the defect  
5 ring, and perform geometric optimization to obtain the optimized structure of the  
6 particles outside the nanotube. Then place the particles inside the nanotube, right above  
7 the defect ring, and perform geometric optimization to obtain an optimized structure of  
8 the particles inside the nanotube. Find the optimal path for particles to pass through the  
9 defect ring from the outside to the inside, and search for the transition state on this path  
10 to obtain the particle diffusion energy barrier. The transition state search includes LST  
11 and QST methods



12

13

Fig. 3 Model of nanotube

14

15

16

17

18

19

20

21

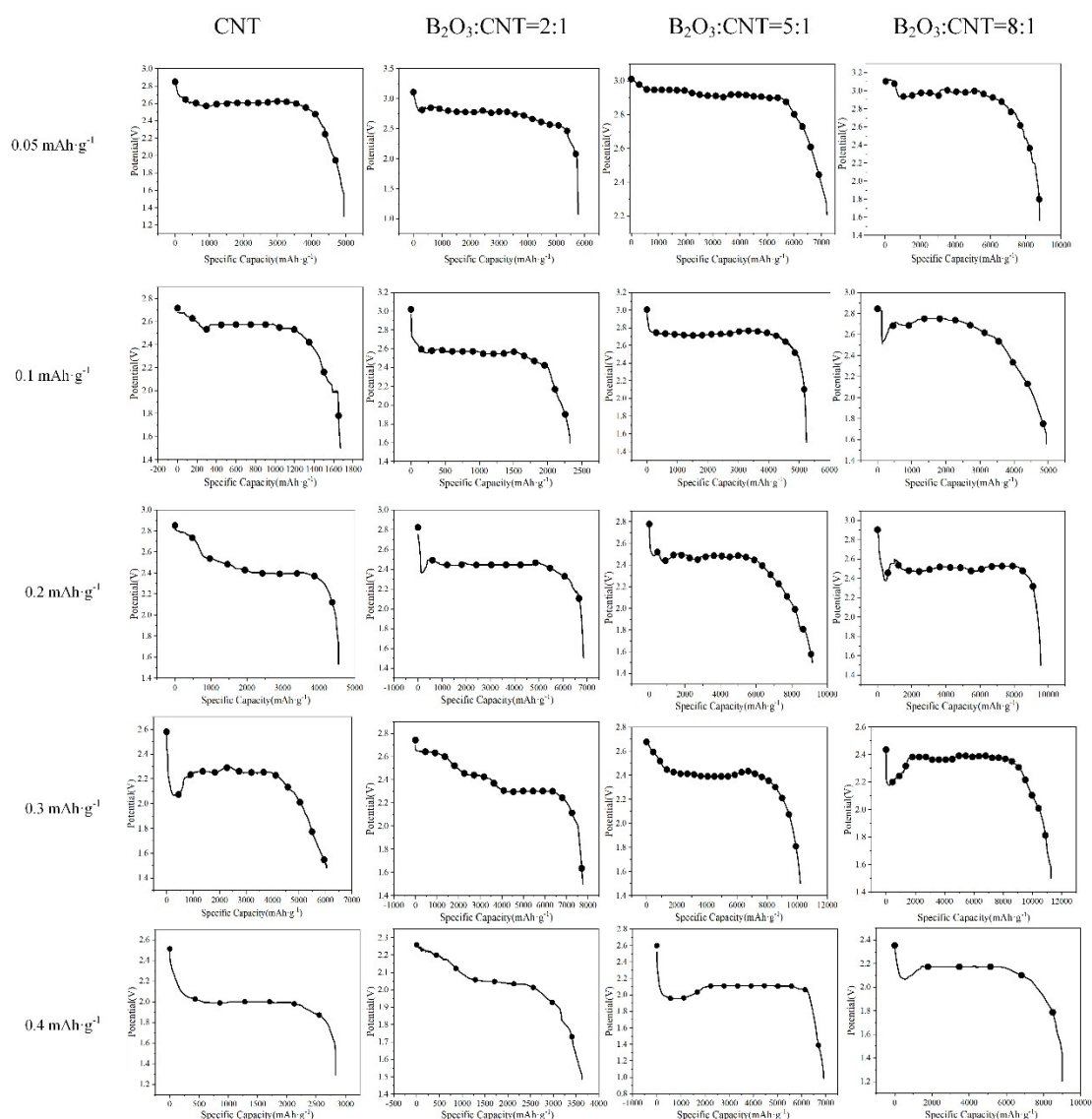
22

23

24

1  
2  
3  
4  
5  
6  
7  
8

## 9 2. Analysis



10  
11  
12  
13  
14

Fig. S2 The deep discharge diagram of the battery.

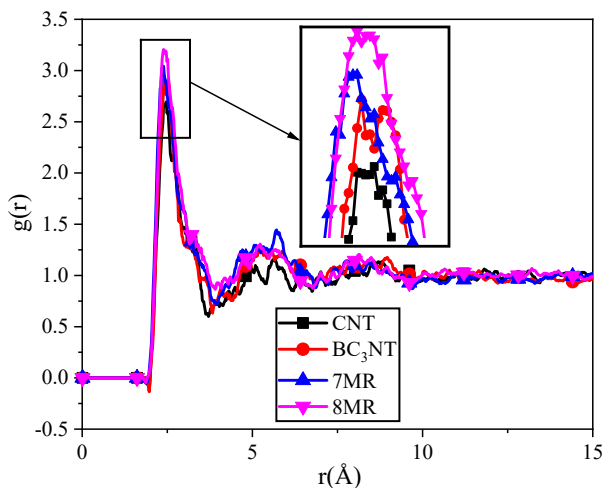
1

Table S2 Impedence of interfacial transfer.

	CNT	B <sub>2</sub> O <sub>3</sub> :CNT=2:1	B <sub>2</sub> O <sub>3</sub> :CNT=2:1	B <sub>2</sub> O <sub>3</sub> :CNT=2:1
Impedence/ $\Omega$	309	283	146	134

2

3

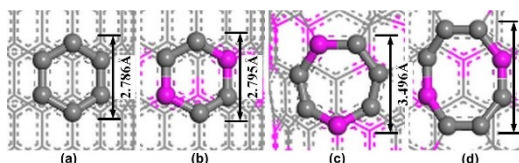


4

Fig. S3 Radial distribution of Li<sup>+</sup>-O<sub>2</sub>.

5

6

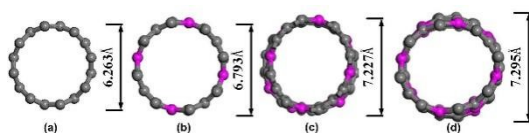


7

Fig. S4 Diameter of nanotube ring: (a)CNT, (b)BC<sub>3</sub>NT, (c)7MR, (d)8MR.

8

9



10

11

Fig. S5 Diameter of nanotubes (a)CNT, (b)BC<sub>3</sub>NT, (c)7MR, (d)8MR.

12

13

14

15

16

17 1 J. Zhou, X. Lu, Y. Wang and J. Shi, *Fluid Phase Equilibria*, 2002, **194–197**, 257–270.18 2 S. Jalili, E. Hosseinzadeh and J. Schofield, *Chemical Physics*, 2014, **438**, 16–22.

19